Role of B800 in Carotenoid–Bacteriochlorophyll Energy and Electron Transfer in LH2 Complexes from the Purple Bacterium Rhodobacter sphaeroides

ARTICLE *in* THE JOURNAL OF PHYSICAL CHEMISTRY B · JULY 2007

Impact Factor: 3.3 · DOI: 10.1021/jp071395c · Source: PubMed

Role of B800 in Carotenoid−Bacteriochlorophyll Energy and Electron Transfer in LH2 Complexes from the Purple Bacterium *Rhodobacter sphaeroides*

Tomáš Polívka,*,†,‡ Dariusz Niedzwiedzki,§ Marcel Fuciman,† Villy Sundström,|| and Harry A. Frank§

Institute of Physical Biology, University of South Bohemia, Zamek 136, CZ-373 33 Nove Hrady, Czech Republic, Biological Centre, Czech Academy of Sciences, Branisovska 31, CZ-370 05 Ceske Budejovice, Czech Republic, Department of Chemistry, University of Connecticut, Storrs, Connecticut 06269-3060, and Department of Chemical Physics, Lund University, Box 124, S-22100 Lund, Sweden

Received: February 19, 2007; In Final Form: April 20, 2007

The role of the B800 in energy and electron transfer in LH2 complexes has been studied using femtosecond time-resolved transient absorption spectroscopy. The B800 site was perturbed by application of lithium dodecyl sulfate (LDS), and comparison of treated and untreated LH2 complexes from *Rhodobacter sphaeroides* incorporating carotenoids neurosporene, spheroidene, and spheroidenone was used to explore the role of B800 in carotenoid to bacteriochlorophyll-*a* (BChl*a*) energy transfer and carotenoid radical formation. Efficiencies of the S_1-mediated energy transfer in the LDS-treated complexes were 86, 61, and 57% in the LH2 complexes containing neurosporene, spheroidene, and spheroidenone, respectively. Analysis of the carotenoid S_1 lifetimes in solution, LDS-treated, and untreated LH2 complexes allowed determination of B800/B850 branching ratio in the S_1-mediated energy transfer. It is shown that B800 is a major acceptor, as approximately 60% of the energy from the carotenoid S_1 state is accepted by B800. This value is nearly independent of conjugation length of the carotenoid. In addition to its role in energy transfer, the B800 BChl*a* is the only electron acceptor in the event of charge separation between carotenoid and BChl*a* in LH2 complexes, which is demonstrated by prevention of carotenoid radical formation in the LDS-treated LH2 complexes. In the untreated complexes containing neurosporene and spheroidene, the carotenoid radical is formed with a time constant of 300−400 fs. Application of different excitation wavelengths and intensity dependence of the carotenoid radical formation showed that the carotenoid radical can be formed only after excitation of the S_2 state of carotenoid, although the S_2 state itself is not a precursor of the charge-separated state. Instead, either a hot S_1 state or a charge-transfer state lying between S_2 and S_1 states of the carotenoid are discussed as potential precursors of the charge-separated state.

1. Introduction

Light-harvesting complexes are vital parts of all photosynthetic organisms extending from bacteria to higher plants. They absorb incident light and transfer the excitation energy to the reaction center where it is converted into chemical energy by a series of electron-transfer steps. Carotenoids assist (bacterio)-chlorophylls [(B)Chl] in the light-harvesting function by absorbing light in the spectral region between 420 and 550 nm and then by transferring the energy to (B)Chl.[1−3] The light-harvesting function of carotenoids is especially important in antenna complexes of purple bacteria because carotenoids efficiently cover the gap between the BChl Soret and Q_x/Q_y bands where BChl only weakly absorbs.

A well-studied purple bacterial light-harvesting complex is the LH2 complex from *Rhodopseudomonas acidophila* whose structure has been determined to 2.0 Å resolution.[4] A similar LH2 complex from *Rhodobacter sphaeroides* has also been investigated in detail. Its X-ray structure is unknown, but on the basis of electron microscopy studies, it is known to have similar structure.[5] The LH2 complexes from these bacteria have a circular structure consisting of nine identical subunits, each one accommodating three BChl*a* molecules and one carotenoid.[6] The carotenoid spans the membrane and comes in close contact with a pair of strongly coupled BChl*a* molecules (B850), forming a ring on one side of the complex and monomeric BChl*a* molecules (B800) oriented parallel with the membrane plane on the other side.[4] This structural knowledge of the LH2 complex has initiated several theoretical and experimental studies of energy transfer pathways.[1,7]

The light-harvesting function of carotenoids in LH2 complexes relies on their ability to transfer energy from their low-lying excited states to both Q_x and Q_y states of BChl*a*. Important roles in carotenoid to BChl*a* energy transfer are played by the S_2 state (denoted $1B_u^+$ according to the C_{2h} symmetry point group), responsible for absorption in 400−550 nm region and also by the one-photon forbidden S_1 state ($2A_g^-$) located a few thousand cm^{-1} below the S_2 state.[1] While these two carotenoid excited states represent the primary energy donors, other excited states denoted $1B_u^-$ and S* have also been suggested to participate in energy transfer between carotenoids and BChl*a* in LH2 complexes.[8−11] Whereas the S_2 and S_1 pathways are now well-established, the exact role of other states in energy transfer still awaits further experimental and theoretical efforts.[1,8,12]

* To whom correspondence should be addressed. Tel: +420 389 033 827. Fax: +420 386 361 219. E-mail: polivka@ufb.jcu.cz.
† University of South Bohemia.
‡ Czech Academy of Sciences.
§ University of Connecticut.
|| Lund University.

10.1021/jp071395c CCC: $37.00
Published on Web 06/05/2007

It has been established that an important factor governing the pathways and efficiencies of energy transfer is the conjugation length of the carotenoid. While the efficiency of energy transfer via S_2 state does not appear to change significantly with conjugation length, usually falling between 40 and 60% regardless of the carotenoid structure,[1,13,14] the efficiency of the S_1-mediated energy transfer in LH2 complexes decreases with increasing π-electron conjugation length of the carotenoid.[15−17] This dependency has been explained in terms of decreasing spectral overlap between S_1 emission and BChl*a* Q_y absorption, as the energy of the S_1 state decreases with increasing conjugation. For carotenoids with several conjugated carbon−carbon double bonds, *N*, greater than 10, the S_1 energy is too low to allow energy transfer via the S_1 pathway. This results in efficiencies of the S_1-channel dropping below 10%.[15−18] Although this explanation is supported by both experimental[15−18] and theoretical[19] studies, recent studies employing reconstituted LH2 complexes suggest that the B800 BChl*a* is a primary energy acceptor in the S_1 pathway. This is especially important in the LH2 complex from *Rps. acidophila*, because its major carotenoid is rhodopin glucoside which has $N = 11$ and an energy too low for efficient S_1-mediated transfer. An approximate 5% efficiency of this channel has been reported.[18,20] Interestingly, however, Macpherson et al. reported that removal of B800 molecule closes the S_1 channel completely, suggesting that the B800 molecule is an energy acceptor even though its Q_y transition has higher energy than that of B850.[18] The significant contribution of the S_1-B800 channel was later confirmed in experiments employing samples having spheroidene incorporated into the LH2 complex from the carotenoidless *Rb. sphaeroides* R26 mutant which lacks the B800 BChl*a*. In this complex, the efficiency of energy transfer via the S_1 pathway was only 35%,[11] which is significantly less than ∼80% observed for the LH2 containing both B800 and B850,[16,20,21] suggesting that the main pathway involves B800 as an acceptor.

In other investigations, B800 has been identified as an electron acceptor in a redox reaction occurring between the carotenoid and BChl*a* in LH2 complexes containing spheroidene and neurosporene after excitation of the S_2 state.[17,20] Formation of the carotenoid radical cation was found to depend on the conjugation length; the shorter the carotenoid, the higher was the yield of carotenoid radical formation reaching 15% for neurosporene with $N = 9$ but only 8% for spheroidene ($N = 10$).[17] No radical formation was observed for carotenoids having $N > 10$, for example, spheroidenone and rhodopin glucoside.[17,20] The mechanism of the carotenoid radical formation in LH2 complexes is still a matter of debate, because the direct precursor of the charge-separated state has not been identified yet.[17,22,23] The 300−400 fs formation time of the carotenoid radical[17] does not match lifetimes of S_2 and S_1 states in LH2 complexes,[1,8,13−18] suggesting that these states cannot be the precursors. Similarly, the S* state cannot be the precursor.[11,24] Therefore, current hypotheses suggest either a higher charge-transfer state[17] or vibrationally hot S_1 state[22] as potential precursors.

In this work, we use femtosecond spectroscopy in the visible and near-infrared regions to investigate both energy and electron transfer in a series of LH2 complexes from *Rb. sphaeroides* having carotenoids with different conjugation lengths. This approach, carried out on samples treated with lithium dodecyl sulfate (LDS), which selectively perturbs the B800 binding site,[25] allowed us to investigate the role of the B800 molecule in the S_1-mediated energy transfer and carotenoid radical formation in LH2 complexes of *Rb. sphaeroides*.

2. Materials and Methods

LH2 complexes of *Rb. sphaeroides* containing neurosporene, spheroidene, or spheroidenone were isolated and purified as described previously.[26,27] The purified LH2 complexes were stored in the dark at −50 °C and just prior to the experiments were suspended in a buffer (50 mM Tris, pH 8, 0.1% LDAO). The preparation of the LH2 complexes reconstituted with spheroidene was done according to previously published procedures.[11] The optical density of all samples was adjusted to 0.1−0.15/mm at the maximum of the 0−0 band of the carotenoid S_0-S_2 transition. The LDS-treated sample was prepared by adding 0.3% LDS (Sigma Aldrich) to the LH2 sample. Prior to the spectroscopic measurements, the sample was incubated in the presence of LDS at room temperature until the B800 band reached a minimum constant amplitude (Supporting Information, Figure S1).

Steady-state absorption measurements were performed on a Jasco-V-530 spectrophotometer in a 2 mm path length quartz cuvette. Ultrafast spectroscopic measurements were carried out at room temperature with the sample in a 2 mm path length quartz rotating cuvette. The femtosecond spectrometer used in this study is based on an amplified Ti:sapphire laser system (Spectra Physics), with tunable pulses obtained from an optical parametric amplifier. The amplified Ti:sapphire laser system was operated at a repetition rate of 5 kHz, producing ∼120 fs pulses with an average output power of ∼1 W and a central wavelength of 800 nm. The amplified pulses were divided into two paths: one to pump an optical parametric amplifier (TOPAS, Light Conversion) for generation of excitation pulses in the spectral range 490−520 nm and the other to produce white-light continuum probe pulses in a 0.3 cm sapphire plate. To prevent sample degradation or annihilation processes in LH2 complexes, the excitation pulses were attenuated to energy of ∼10 nJ/pulse by means of neutral density filters. To obtain excitation at 395 nm, the amplified pulses were tuned to 790 nm and then were frequency-doubled using a BBO crystal. The pump and probe pulses were allowed to overlap at the sample placed in a quartz rotating cell. The pump beam was focused to a spot size of ∼300 μm in diameter, corresponding to a photon density of $\sim 2 \times 10^{13}$ photons·cm^{-2}·pulse^{-1}. The intensity dependence experiments were carried out in the range of excitation photon densities of $0.6-13 \times 10^{13}$ photons·cm^{-2}·pulse^{-1}. The actual intensity was adjusted by neutral density filters. The mutual polarization of pump and probe beams was set to the magic angle (54.7°). Absorption spectra were measured before and after the ultrafast measurements to ensure that no photodamage to the samples occurred over the duration of the experiments.

3. Results

Absorption Spectra. The absorption spectra of the LH2 complexes are shown in Figure 1. For the untreated complexes, the line shapes are dominated by the two characteristic BChl*a* bands peaking at 800 nm (B800 band) and 850 nm (B850 band), accompanied by a weaker BChl*a* Q_x band centered at 590 nm. The position of these bands is, within 1 nm, the same for all the untreated LH2 complexes indicating negligible effect of the carotenoid on the position of the BChl*a* absorption bands. Significant differences between the untreated LH2 complexes are observed in the carotenoid region, since the position of the absorption bands is determined by the conjugation length of the carotenoid. It varies from $N = 9$ (neurosporene) to 10 (spheroidene) and 10 + C═O (spheroidenone). The lowest energy carotenoid bands corresponding to the 0−0 vibrational

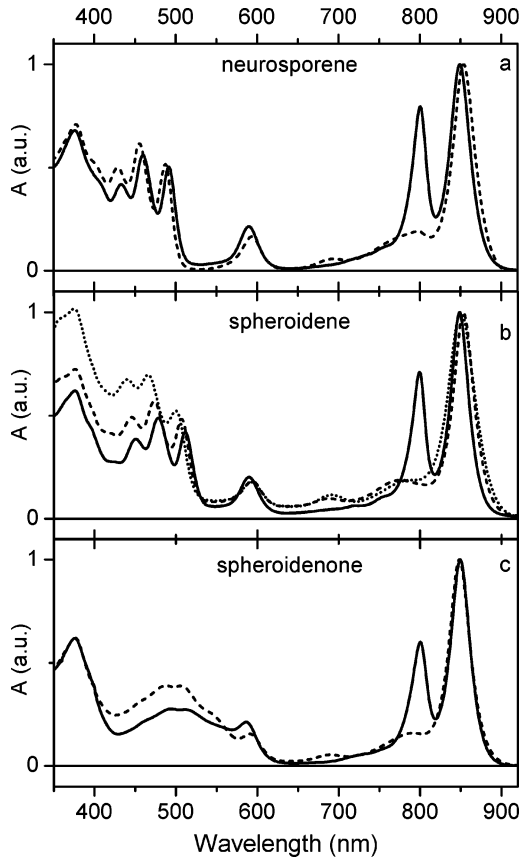

Figure 1. Absorption spectra of the LH2 complexes containing the carotenoid neurosporene (a), spheroidene (b), and spheroidenone (c). Solid lines represent absorption spectra of the untreated LH2 complexes, while dashed lines are the spectra obtained after 120 min of treatment with 0.3% LDS. In panel b, the absorption spectrum of the spheroidene-reconstituted complex is also shown (dotted line).

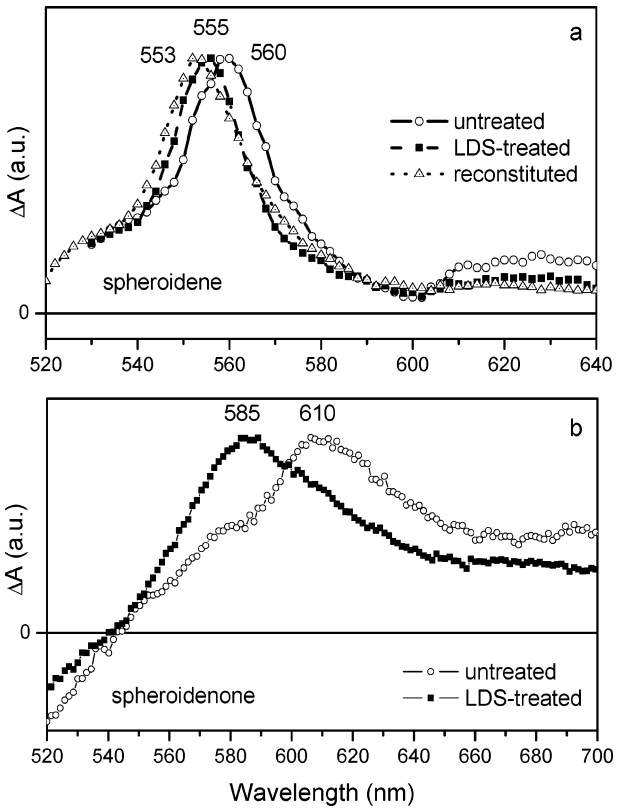

Figure 2. Transient absorption spectra of the LH2 complexes containing spheroidene (a) and spheroidenone (b) obtained 1 ps after excitation of the carotenoid at 515 nm (spheroidene) and 520 nm (spheroidenone). Transient absorption spectra were measured for the untreated LH2 complexes (open symbols) and for LDS-treated LH2 complexes (full symbols). The transient absorption spectrum of the spheroidene-reconstituted complex is also shown (open triangles in panel a). All spectra are normalized to the maximum band intensity.

transitions of the S_2 state are located at 492 nm (neurosporene), 512 nm (spheroidene), and 515 nm (spheroidenone). The vibrational bands of the S_2 state are markedly sharper in the LH2 complexes containing neurosporene and spheroidene. Substantial broadening of the S_0-S_2 absorption of spheroidenone is due to the presence of the conjugated carbonyl group.[28,29] Treatment of the LH2 complexes by LDS leads to about 80% depletion of the B800 band (see Supporting Information for the time course of the LDS-induced changes) and is accompanied by the appearance of weak spectral bands around 770 and 680 nm.[25] In addition, the LDS treatment results in spectral shifts of both the B850 band and the carotenoid S_2 band. The B850 pigment exhibits a 3−4 nm red shift[25] that is clearly observed in Figure 1 for the LDS-treated LH2 complexes containing neurosporene and spheroidene. For the spheroidenone-containing LH2 complex, however, the LDS treatment does not produce any observable shift, and despite the depletion of the B800 band, the B850 band is nearly identical for the untreated and LDS-treated LH2 complex (Figure 1c). In the carotenoid region, the LDS treatment induces an approximate 5 nm blue shift of the 0−0 transition of the carotenoid S_2 state for all LH2 complexes. We have also carried out measurements on a spheroidene-reconstituted LH2 complex, for which the spheroidene S_2 band is further blue-shifted, indicating less interaction between the protein and carotenoid. In general, the stronger the carotenoid−protein interaction, the more red-shifted is the S_2 absorption band.

Transient Absorption in the Visible Region. The LH2 antenna complexes were excited in the 0−0 vibronic band of the carotenoid absorption at 490 nm (neurosporene), 515 nm (spheroidene), and 520 nm (spheroidenone). Transient absorption spectra recorded 1 ps after excitation, which monitor the S_1-S_N transition of carotenoids,[1] are shown in Figure 2. For the LH2 complex containing spheroidene, the changes in the transient absorption spectra are reminiscent of those observed in the steady-state absorption. The LDS treatment induces a blue shift of the S_1-S_N band to 555 nm compared with the 560 nm maximum for the untreated complex. A similar effect is observed also for neurosporene (data not shown). An additional blue shift to 553 nm appears for the LH2 complex reconstituted with spheroidene, confirming the somehow diminished carotenoid−protein interaction in this sample. An even larger blue shift is observed for the LH2 complex containing spheroidenone. For the untreated complex, the S_1-S_N band of spheroidenone peaks at 610 nm but shifts to 585 nm following LDS treatment. Thus, while the S_0-S_2 transition of spheroidenone exhibits only a 5 nm shift upon the LDS-treatment, the S_1-S_N band undergoes a much larger shift of 25 nm. The significant difference between the LDS-induced shifts of the S_0-S_2 and S_1-S_N transitions of spheroidenone indicates that the removal of the B800 BChl*a* molecule has a larger effect on the S_1 state of spheroidenone perhaps related to its coupling to a charge-transfer state arising from the conjugated carbonyl group of the carotenoid. Because of this coupling, the S_1 state properties are sensitive to the properties of environment,[28,29] and the removal of B800 may affect the immediate environment of the carbonyl group, leading to the observed large LDS-induced shift of the S_1-S_N transition for this sample.

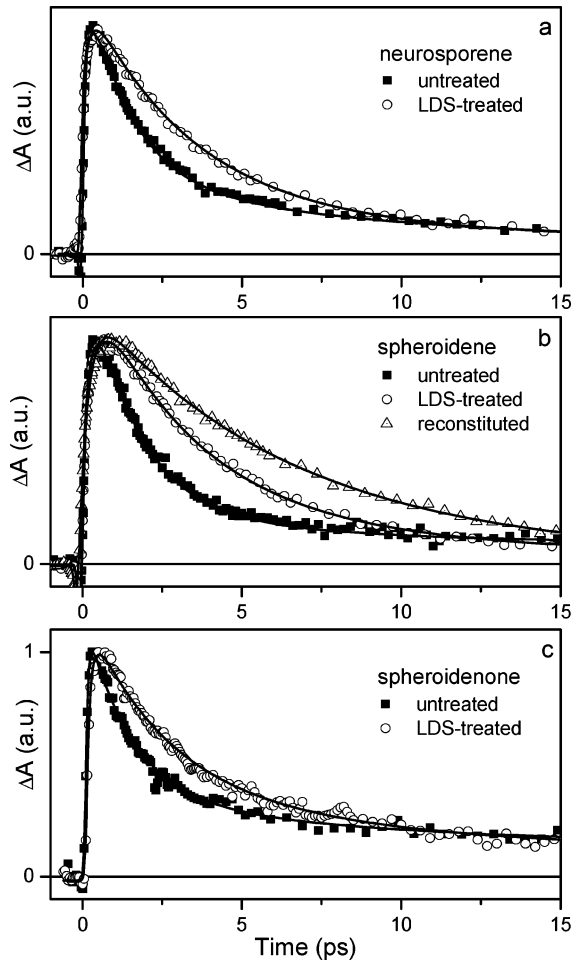

Figure 3. Kinetics recorded at the maximum of the S_1-S_N band for the untreated and LDS-treated LH2 complexes containing neurosporene (a), spheroidene (b), and spheroidenone (c). For spheroidene, the reconstituted LH2 complex is also shown (open triangles). The LH2 complexes were excited in the carotenoid region at 490 nm (neurosporene), 515 nm (spheroidene), and 520 nm (spheroidenone). All kinetics are normalized to the maximum. Solid lines represent fits.

The lifetimes of the carotenoid S_1 state in the LH2 complexes were obtained from kinetics measured at probe wavelengths corresponding to the maximum of the S_1-S_N band. Kinetics from both untreated and LDS-treated LH2 complexes are shown in Figure 3. In agreement with previous analyses performed on untreated LH2 complexes,[11,16,17] at least three components are needed to fit the kinetics (see Table 1 for summary). The first component is necessary to fit the rise of the S_1-S_N signal, and its time constant is in the range of 0.1−0.15 ps for the untreated complexes. This is longer than the sub-100 fs S_2 lifetimes obtained from either fluorescence up-conversion measurements[13,14,18] or global fitting of transient absorption data.[10] The reason for this discrepancy lies in the fact that the kinetics measured at the maximum of the S_1-S_N band unavoidably contains also a contribution from S_1 vibrational relaxation that is longer than the S_2 lifetime.[30,31] Thus, the rise component obtained from the kinetics at this wavelength represents a mixture of the S_2 lifetime and vibrational relaxation. This results in a longer time constant than should be the case for the pure S_2 state lifetime. The rise components are systematically longer for the LDS-treated LH2 complexes. This indicates longer S_2 lifetime that reflects reduction in energy transfer efficiency of the S_2 channel in the LH2 complexes lacking the B800 acceptor (Table 1).

TABLE 1: Time Constants Obtained from Fitting of the S_1-S_N Decays[a]

LH2 complex	τ_{rise} (ps)	τ_1 (ps)	A_2 (%) $\tau_2 = 9$ ps	A_3 (%) $\tau_3 = >500$ ps
neurosporene	0.1 (−86)	1.4 (74)	22	4
neurosporene−LDS	0.22 (−48)	3.1 (80)	16	4
spheroidene	0.16 (−59)	1.6 (95)	2	3
spheroidene−LDS	0.37 (−68)	3.4 (84)	13	3
spheroidene−Rec	0.27 (−80)	6.0 (82)	15	3
spheroidenone	0.11 (−67)	1.5 (80)	18	2
spheroidenone−LDS	0.14 (−78)	2.6 (66)	20	14

[a] Amplitudes of the first two components are given in parentheses. The other two components were fixed during the fitting procedure. Negative amplitudes represent a rise component, while positive amplitudes correspond to a decay. For the rise component, τ_{rise}, the amplitude remaining to −100% is due to instantaneous rise.

The main decay component corresponds to the carotenoid S_1 lifetime. For the untreated LH2 complexes, the S_1 lifetime is essentially independent of the carotenoid yielding values of 1.4 ps (neurosporene), 1.6 ps (spheroidene), and 1.5 ps (spheroidenone). For the LDS-treated complexes, however, the S_1 lifetimes become systematically longer and the extracted time constants are 3.1 ps (neurosporene), 3.4 ps (spheroidene), and 2.6 ps (spheroidenone). Even after the LDS-treatment that results in removal of the B800 BChl*a*, the S_1 lifetimes remain significantly shorter than those measured for these carotenoids in solution. The values in *n*-hexane solution are 24, 8.5, and 6 ps for neurosporene, spheroidene, and spheroidenone. The difference indicates presence of S_1-mediated energy transfer also for the LDS-treated complexes. For the LH2 complex reconstituted with spheroidene, the S_1 lifetime is 6 ps. For all complexes besides the dominant component associated with the S_1 lifetime, acceptable fits cannot be obtained without including an additional longer component of about 9 ps. This is most likely due to a contribution of the S* state.[10,11] Also, a nondecaying component that accounts for a weak BChl*a* excited-state absorption in the visible spectral region is observed.

Transient Absorption in the Near-IR Region. While the measurements in the visible spectral region provide information about the lifetime of the carotenoid S_1 state, probe wavelengths in the near-IR region follow LDS-induced effects on the B850 BChl*a* and formation of the carotenoid radical which displays a distinct absorption band in the 900−1000 nm region.[32] The effect of LDS on the near-IR transient absorption spectra of the LH2 complex containing neurosporene was analyzed in detail in a previous study.[17] Here, we focus on the LH2 complexes containing spheroidene and spheroidenone whose near-IR transient absorption spectra were recorded with and without LDS (Figure 4). The position of the B850 bleaching mirrors the subtle LDS-induced red shift observed in the absorption spectrum of the spheroidene-containing LH2 complex. In agreement with the absorption spectra shown in Figure 1, the position of the B850 bleaching for the LH2 complex with spheroidenone is identical regardless of whether the LDS is present or not. Kinetics of the B850 rise monitors energy transfer from the carotenoid (Figure 5). Similar to the S_1-S_N kinetics shown in Figure 3, the presence of LDS results in a slower B850 rise indicating less-efficient energy transfer in the complexes lacking the B800 BChl*a*. Contrary to the S_1-S_N decay, however, the analyses of the B850 rise are complicated. For the untreated complexes due to the S_2-mediated energy transfer that occurs to both B800 and B850 molecules,[18,21] an additional component representing B800−B850 energy transfer will be also present.

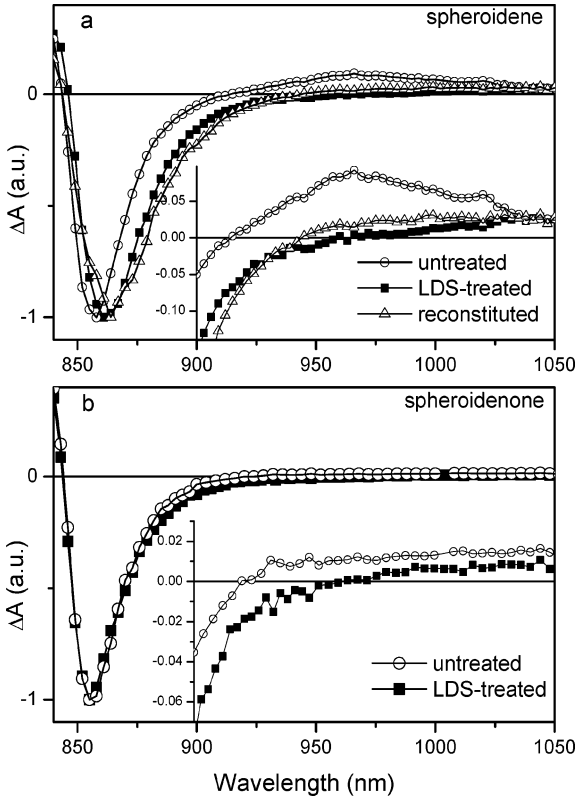

Figure 4. Transient absorption spectra of the LH2 complexes containing spheroidene (a) and spheroidenone (b) in the near-IR region. Transient absorption spectra were measured 1 ps after excitation for the untreated LH2 complexes (open circles) and for the LDS-treated LH2 complexes (full squares). The spheroidene-reconstituted LH2 complex is also shown (open triangles in panel a). Insets show the enlargement of the region of the carotenoid radical absorption. All spectra are normalized to the minimum of the B850 bleaching. Excitation was at 515 nm (spheroidene) and 520 nm (spheroidenone).

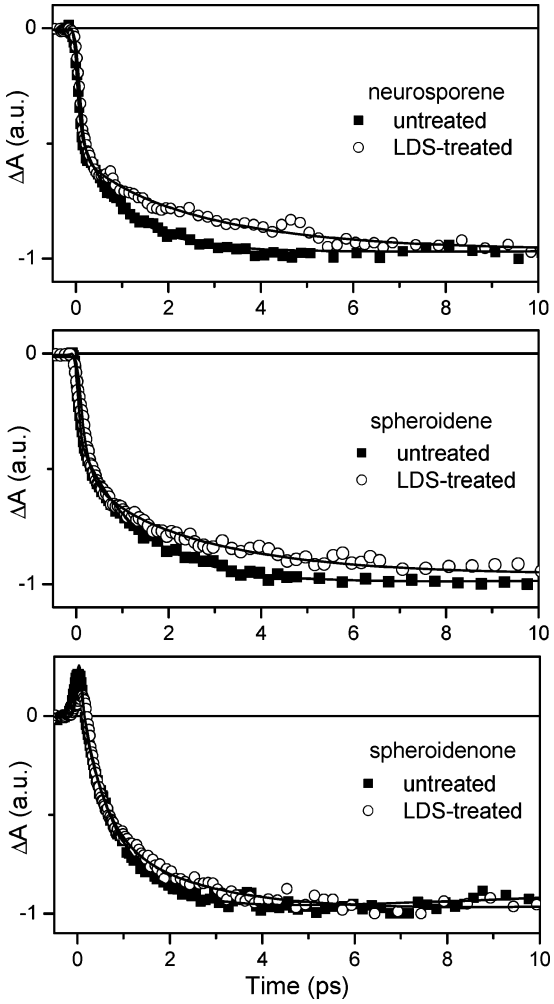

Figure 5. Kinetics of the B850 rise for untreated (full squares) and LDS-treated (open circles) LH2 complexes. Kinetics are normalized to the minimum signal amplitude. The samples were excited at 490 nm (neurosporene), 515 nm (spheroidene), and 520 nm (spheroidenone). Fits are shown as solid lines.

Consequently, the untreated LH2 complexes were fitted with an additional rise component whose time constant was fixed at 0.7−0.8 ps, the reported range for B800−B850 energy transfer.[7] Because the B800 is removed by LDS, the B850 rise for the LDS-treated LH2 complexes was fitted with only two rise components: a fast (<200 fs) rise that must be present because of the S_2-mediated energy transfer and another component corresponding to the energy transfer from the S_1 state of the carotenoid. The fitting results are summarized in Table 2. The time constants of the S_1-mediated energy transfer match reasonably well those extracted from the fitting of the S_1-S_N decays listed in Table 1.

In the region of the carotenoid radical absorption (insets in Figure 4), the spectra are comparable with those obtained earlier for the neurosporene-containing LH2 complex.[17] A spheroidene radical band peaking at 960 nm is observed. Similar to the LH2 complex with neurosporene, the LDS-treatment prevents the carotenoid radical from being formed in the spheroidene-containing LH2 complex. The same result is obtained also for the B850-only LH2 complex reconstituted with spheroidene, again emphasizing the key importance of the B800 BChl*a* for carotenoid radical formation.[17,20] The effect of LDS on the formation of the spheroidene radical in the LH2 complex is further manifested in the kinetics measured at the wavelength corresponding to the maximum of the radical signal. The kinetics recorded at 960 nm for the untreated and LDS-treated LH2 complexes with spheroidene are shown in Figure 6a. In both kinetic traces, the initial fast decrease of the signal is due to a decay of the S_2-S_N absorption (<0.15 ps) that has substantial amplitude in this spectral region.[24,33] For the untreated complex, the kinetic traces contain a slower component with a time constant of 8 ps that is assigned to the decay of the spheroidene radical. The fitting reveals also a 300 fs rise of the radical signal (Figure 6a) that indicates that the spheroidene radical is not formed directly from the S_2 state (see Discussion and ref 17). After the LDS-treatment, the S_2 decay forms a negative signal that is due solely to the red tail of the B850 bleaching (see transient absorption spectrum in Figure 4), and no signal attributable to the spheroidene radical is observed.

TABLE 2: Time Constants Obtained from Fitting of the Rise of the B850 Bleaching[a]

LH2 complex	τ_1 (ps)	τ_2 (ps)
neurosporene	1.5 (−20)	0.8 (−40)
neurosporene−LDS	3.2 (−43)	
spheroidene	1.4 (−53)	0.7 (−8)
spheroidene−LDS	3.3 (−48)	
spheroidenone	1.5 (−20)	0.7 (−47)
spheroidenone−LDS	2.8 (−53)	

[a] Numbers in parentheses correspond to the amplitudes of the time components. The amplitude remaining to −100% is due to instantaneous rise.

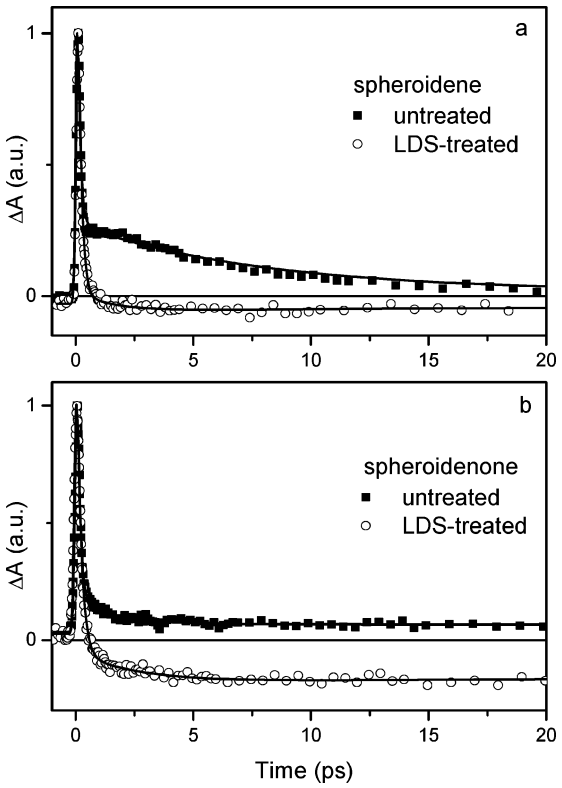

Figure 6. Kinetics recorded at the maximum of the carotenoid radical absorption, 960 nm, for the untreated (solid squares) and LDS-treated (open circles) LH2 complexes containing spheroidene (a) and spheroidenone (b). Kinetics are normalized to maximum. Excitation at 515 nm (spheroidene) and 520 nm (spheroidenone).

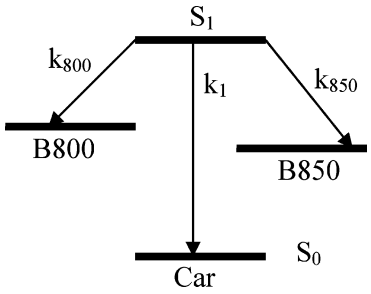

Figure 7. Schematic diagram showing the possible relaxation and energy transfer pathways from the S_1 state of a carotenoid in LH2. Each pathway is denoted by a corresponding rate constant.

4. Discussion

Role of the B800 in Carotenoid−BChl*a* Energy Transfer. Selective perturbation of the B800 binding site by LDS treatment gives an opportunity to explore the role of the B800 molecule in carotenoid−BChl*a* energy transfer in LH2 complexes. Since for the carotenoids studied here the S_1 lifetimes are independent of environment,[1,28,29] comparison of the carotenoid S_1 lifetimes in LH2 complexes with known carotenoid S_1 lifetimes in solution allows a determination of the S_1-mediated energy-transfer efficiency and energy transfer rates. For untreated LH2 complexes, the S_1 relaxation channels are schematically depicted in Figure 7. The total decay rate of the S_1 state, k, in the LH2 complex is

$$k = k_1 + k_{800} + k_{850} = k_1 + k_{ET} \quad (1)$$

where $k_{ET} = k_{800} + k_{850}$ represents the decay rate caused by energy transfer to BChl*a*. Thus, using the values of $\tau_1 = k_1^{-1}$ for the S_1 lifetimes of carotenoids in solution, it is possible to calculate the energy transfer time τ_{ET} according to the equation

$$\tau_{ET} = \left(\frac{1}{\tau} - \frac{1}{\tau_1}\right)^{-1} \quad (2)$$

where $\tau = k^{-1}$ is the carotenoid S_1 lifetime in LH2 obtained from experiment. Then, efficiency of the S_1-mediated energy transfer is calculated from equation

$$\phi_{ET} = \frac{k_{ET}}{k_1 + k_{ET}} = \frac{k - k_1}{k_1 + k_{ET}} = \frac{k - k_1}{k} = 1 - \frac{k_1}{k} = 1 - \frac{\tau}{\tau_1} \quad (3)$$

Since the B800 acceptor is missing in the LDS-treated LH2 complexes, $k_{ET} = k_{B850}$ for these complexes under assumption that k_{B850} is not changed by LDS-treatment. Since the B850 binding site is not affected by the removal of the B800 BChl*a*,[34] this assumption is justified. Consequently, using the τ values obtained for the untreated and LDS-treated complexes allows for calculation of τ_{800}, the energy transfer time for the carotenoid−B800 energy transfer as follows

$$\tau_{800} = \left(\frac{1}{\tau} - \frac{1}{\tau_{LDS}}\right)^{-1} \quad (4)$$

where τ and τ_{LDS} are the measured S_1 lifetimes of carotenoids in untreated and LDS-treated LH2 complexes, respectively. Knowledge of τ_{800} gives the efficiency of carotenoid−B800 energy transfer and thus, the B800/B850 branching ratio for the S_1-mediated energy transfer in LH2:

$$\phi_{B800} = \frac{k_{800}}{k_{ET}} = \frac{\tau_{ET}}{\tau_{800}} \quad (5)$$

Values obtained from the analysis described above are summarized in Table 3. For the untreated LH2 complexes, the S_1-mediated energy transfer efficiencies are 94% (neurosporene), 82% (spheroidene), and 75% (spheroidenone), all in good agreement with previously reported values.[16,17] For the LDS-treated complexes, the efficiency of the S_1-mediated energy transfer decreases, yielding values of 86% (neurosporene), 61% (spheroidene), and 57% (spheroidenone), showing that the B800 removed by the LDS treatment is contributing to the S_1-mediated energy transfer. The importance of the B800 molecule is even more noticeable by a comparison of the S_1-B850 and S_1-B800 energy transfer times. The values of τ_{ET} for the LDS-treated complexes correspond to the S_1-B850 energy transfer times (Table 3). These values are 3.6 ps (neurosporene), 5.7 ps (spheroidene), and 4.6 ps (spheroidenone). For all three carotenoids, the S_1-B850 transfer times are slower than the S_1-B800 energy transfer times calculated from eq 4 which gives 2.6 ps (neurosporene), 3.1 ps (spheroidene), and 3.5 ps (spheroidenone). Consequently, the B800 molecule is the primary acceptor of energy in the S_1-mediated pathway of carotenoid to BChl*a* energy transfer. This is further evidenced by the B800/B850 branching ratios obtained from eq 6: 58% of energy transferred from the S_1 state of neurosporene goes to B800. For spheroidene and spheroidenone, these values yield 64% and 57%, respectively (Table 3).

The dominance of the B800 channel is in accord with previous studies using B850-only LH2 complexes reconstituted with different carotenoids.[11,15] Comparison of the LDS-treated and reconstituted LH2 complex with spheroidene studied here, however, shows that reconstitution may overestimate the role of B800 molecule. The S_1-B850 energy transfer times obtained here for the LDS-treated and reconstituted LH2 complexes are

TABLE 3: Parameters of Energy Transfer in LH2 Complexes[a]

LH2 complex	τ (ps)	τ_1[b] (ps)	τ_{ET} (ps)	Φ_{S1}	τ_{800} (ps)	B800/B850
neurosporene	1.4 ± 0.2	22.6 ± 1.4	1.5 ± 0.2	0.94 ± 0.02	2.6 ± 0.8	58/42
neurosporene−LDS	3.1 ± 0.3	22.6 ± 1.4	3.6 ± 0.4	0.86 ± 0.02		
spheroidene	1.6 ± 0.2	8.8 ± 0.7	2.0 ± 0.3	0.82 ± 0.04	3.1 ± 0.9	64/36
spheroidene−LDS	3.4 ± 0.4	8.8 ± 0.7	5.7 ± 1.2	0.61 ± 0.07		
spheroidene−Rec	6.0 ± 0.7	8.8 ± 0.7	25 ± 12	0.30 ± 0.12		
spheroidenone	1.5 ± 0.2	6.0 ± 1.0	2.0 ± 0.5	0.75 ± 0.06	3.5 ± 1.0	57/43
spheroidenone−LDS	2.6 ± 0.3	6.0 ± 1.0	4.6 ± 1.0	0.57 ± 0.10		

[a] Values of total energy transfer time via the S_1 channel (τ_{ET}), efficiency of the S_1 channel (Φ_{S1}), energy transfer time via the S_1-B800 channel (τ_{800}), and branching ratio between the B800 and B850 acceptors (B800/B850) are calculated from the carotenoid S_1 lifetime in LH2 complexes (τ) and in solution (τ_1) according to eqs 2−5. [b] In *n*-hexane. The values correspond to an average of the S_1 lifetimes published in the literature.

5.7 and 25 ps (Table 3), respectively, indicating that reconstituted LH2 complexes likely have weaker coupling between the carotenoid and the B850 BChl*a*. Weaker coupling may be also deduced from both absorption and transient absorption spectra shown in Figures 1b and 2a; the protein-induced shift of the spheroidene bands is less for the reconstituted LH2 complex, suggesting weaker spheroidene−protein interaction.

Interestingly, the B800/B850 branching ratio is not affected by the conjugation length of the carotenoid. Even for spheroidenone having an S_1 energy of $\sim$13 000 cm^{-1},[29] the S_1-B800 pathway remains dominant. This observation does not match values expected from calculations.[19,21] Also, comparison of the efficient S_1-channel observed for spheroidenone with the nearly zero efficiency of this channel obtained for LH2 complexes with rhodopin glucoside that have S_1 energies of 12550 ± 150 cm^{-1} [20] would imply that an $\sim$500 cm^{-1} decrease in the carotenoid S_1 energy is enough to completely close the S_1-B800 pathway. Taking into account that the S_1 emission of carotenoids is quite broad,[35,36] such a drop can be hardly explained solely by a change in spectral overlap.[3,21] Thus, it indicates that other factors besides conjugation length may play a role. A possible explanation was offered by Ritz et al. who noted that the conjugated systems of neurosporene and spheroidene, which systematically exhibit highly efficient energy transfer via the S_1 state, have a non-C_{2h}-symmetrical arrangement of their methyl side groups.[3] This is, however, not the case for lycopene and rhodopin glucoside, both exhibiting very low efficiencies of the S_1-mediated energy transfer.[16−18,37] Consequently, Ritz et al.[3] suggested phenomenologically that the symmetry breaking of neurosporene and spheroidene may be an important factor in explaining why energy transfer via the S_1 state is much more efficient for these carotenoids compared to lycopene and rhodopin glucoside. Since the conjugated system of spheroidenone has also asymmetric arrangement of methyl groups, the observation of active S_1-B800 channel in the spheroidenone-containing LH2 complex provides further support for the conjecture proposed by Ritz et al.[3]

Role of B800 in Electron Transfer. In our previous paper on the carotenoid radical formation in LH2 complexes,[17] we used the LDS treatment to demonstrate that a perturbation of the B800 site in neurosporene-containing LH2 complexes prevents formation of the neurosporene radical cation. This result, in combination with observation of the BChl*a* anion band, led to the conclusion that neurosporene radical is formed via charge separation between neurosporene and B800 BChl*a*. Extension of the LDS treatment to the LH2 complexes with other carotenoids presented here confirms this assignment. For the spheroidene-containing LH2 complex, the LDS treatment removes the characteristic signal of the spheroidene radical cation at 960 nm (Figure 6a), indicating that perturbation of the B800 site prevents the carotenoid radical formation regardless of the structure of the carotenoid. The spheroidene radical is not observed either in the LDS-treated or reconstituted LH2 complexes, confirming that the LDS treatment is equivalent to the selective removal of the B800 BChl*a*.

The interpretation of the LDS effect in this spectral region for the LH2 complex containing spheroidenone is less obvious (Figures 4b and 6b). For the untreated complex, the initial fast decay again reflects the S_2 lifetime via decay of the S_2-S_N transition, but there is no clear radical signal. Consequently, on the basis of the results on untreated complexes, it was proposed that spheroidenone cannot be oxidized in LH2.[17] A direct comparison of the LDS-treated and untreated complexes shown in Figures 4 and 6 favors this interpretation, but there is a clear difference in the spectral region of the carotenoid radical between the untreated and LDS-treated LH2 complexes. Thus, one may interpret the positive signal around 950 nm for the untreated complex as because of a weak spheroidenone radical signal because efficiency of the carotenoid radical formation in LH2 decreases with increasing conjugation length.[17] However, the position of the carotenoid radical spectral band shifts to longer wavelength with increasing conjugation length. Thus, the observed radical peaks of neurosporene at 935 nm[17] and spheroidene at 960 nm (Figure 4a) put the expected maximum for the spheroidenone radical somewhere around 980−990 nm. This rules out the assignment of the residual signal to the spheroidenone radical. The formation of spheroidenone radical was recently also excluded on the basis of calculations.[22] Thus, the difference between the untreated and LDS-treated LH2 complexes containing spheroidenone is most likely because of the slightly broader B850 absorption band of the LDS-treated LH2 complexes (Figure 1c) that moves the zero-crossing point in the transient absorption spectra toward longer wavelength. This interpretation is also supported by the kinetics measured at 950 nm (Figure 6b) that, except for the magnitude of the final plateau, exhibit identical dynamics. No additional component attributable to the decay of spheroidenone radical is observed.

It appears that the only way to initiate the carotenoid−B800 charge separation is by direct excitation of the carotenoid. Excitation into the B850, B800, or even Q_x band of BChl*a* did not produce the charge-separated state.[17,20] While the absence of charge separation after B850 and B800 excitation was explained on the basis of energetic reasons,[17,22] the lack of radical production following excitation of the Q_x band is less obvious as its energy is clearly above that of the charge-separated state. Accordingly, it was proposed that the charge-separated state is formed via a charge-transfer state precursor located above the Q_x state.[17] To test this hypothesis, we have measured transient absorption spectra in the spectral region of the carotenoid radical after excitation of the Soret band of BChl*a* at 395 nm. We have chosen the spheroidene-containing LH2 complexes, because contribution of the spheroidene absorption is small at 395 nm (Figure 1b). Comparison of transient

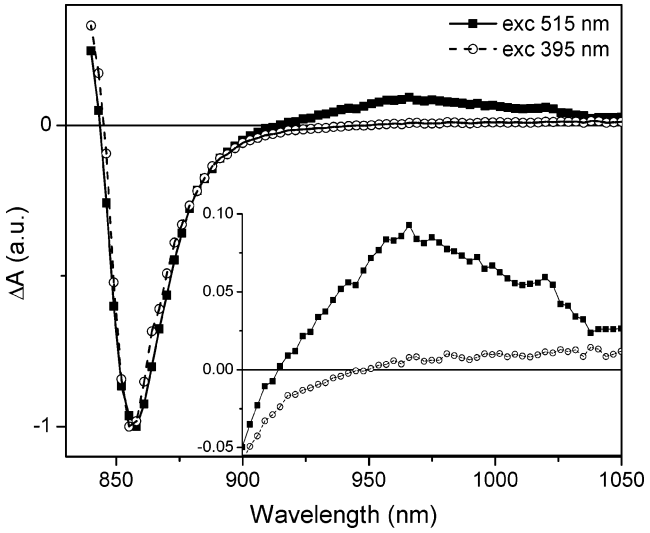

Figure 8. Transient absorption spectra in the near-IR region for the untreated LH2 complexes containing spheroidene measured 1 ps after excitation at 515 nm (full symbols) and 395 nm (open symbols). Inset shows enlargement of the carotenoid radical region. Spectra are normalized to the B850 bleaching.

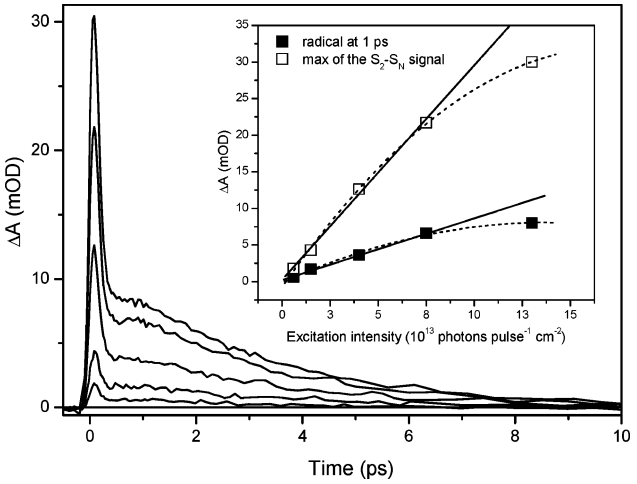

Figure 9. Intensity dependence of the kinetics probed at 930 nm for the LH2 complex containing neurosporene. Excitation wavelength 490 nm. Excitation intensities were 0.6, 1.5, 4, 7.5, and 13×10^{13} photons pulse^{-1} cm^{-2}. Inset shows dependence of signal magnitude at the S_2-S_N maximum (open symbols) and at 1 ps (full symbols) on excitation intensity. Solid lines represent linear fits, while the broken lines are fits to the second-order polynomial function.

absorption spectra obtained after 395 nm (red wing of the BChl*a* Soret band) and 515 nm (0−0 band of the spheroidene S_2 state) excitation shown in Figure 8 clearly indicates that excitation of the Soret band does not produce the charge-separated state either. This is further confirmed by kinetics measured at 960 nm (Supporting Information, Figure S2); while the 515 nm excitation gives significant contribution from the radical signal, the shape of the kinetics taken after 395 nm excitation resembles the rise of the B850 bleaching, except for the weak initial excited-state absorption signal that is due to the residual spheroidene S_2-S_N transition. Thus, the excitation of the Soret band produces no radical, and the observed dynamics reflects solely the rise of the very red edge of the B850 band.

Our analysis shows that even excitation of BChl*a* states that are located higher in energy than the carotenoid S_2 state cannot form the carotenoid radical. This may invoke the question of whether the precursor of the carotenoid radical in LH2 is at all produced from a state that lies below the carotenoid S_2 state, because recent experiments on carotenoids demonstrated that some dynamics can be caused by two-photon processes populating higher-lying states.[12,38] To explore this possibility, we have measured excitation intensity dependence of the carotenoid radical formation in the LH2 complex containing neurosporene. This sample exhibits the highest yield of the carotenoid radical formation. Kinetics measured at 930 nm (maximum of the neurosporene radical) at different excitation intensities are shown in Figure 9. Plotting the magnitude of the radical signal as a function of excitation intensity should reveal the presence of any potential nonlinear processes. The resulting intensity dependencies of both the radical signal at 1 ps and the maximum of the S_2-S_N signal are shown in the inset of Figure 9. Both data sets may be fitted linearly except the data point corresponding to the highest excitation intensity for which the dependence begins to exhibit saturation behavior. The important observation is that both the S_2-S_N and radical signal exhibit identical dependencies on excitation intensity. Since the S_2-S_N signal is formed directly by the excitation of the carotenoid S_2 state, while the radical is created by a subsequent process involving other states, the observation of identical, nearly linear intensity-dependent behavior excludes the possibility of the charge-separated state being formed by a nonlinear process. Except for the intensity-dependent experiment, all excitation intensities used for the data presented here were nearly one order of magnitude below the point of deviation from the linear dependence shown in Figure 9. Therefore, carotenoid radical in LH2 is not produced via two-photon processes involving higher excited states.

The direct precursor of the carotenoid radical as well as the function of any of this radical in LH2 remains unclear. The 300−400 fs formation time of the carotenoid radical[17] precludes the S_2, S_1, and S* states of carotenoid as potential precursors because no corresponding time component was ever observed in their decays. There are two hypotheses concerning the precursor of the charge-separated state. The first possibility is the hot S_1 state suggested by Wormit and Dreuw.[22] While the observed depopulation times of the hot S_1 state in LH2 complexes roughly match the formation times of the carotenoid radical, the contribution of the hot S_1 state to the overall dynamics in LH2 complexes is significantly less than the known yield of the carotenoid radicals.[10,39] Additional weakness of this hypothesis is the fact that the covalent-type states such as the S_1 state (the states with minus pseudoparity sign, the S_1 state has $1A_g^-$ symmetry) are expected to be worse electron donors than the ionic-type states (e.g., $1B_u^+$)[40] as demonstrated, for example, by absence of electron injection from the S_1 state when a carotenoid was attached to a semiconductor surface.[41] The second hypothesis is the existence of a charge-transfer state located just below the S_2 state of carotenoid that serves as a precursor to the final charge-separated state Car^+-B800^-.[17] This hypothesis is based on density functional theory calculations showing that a few such states may be indeed located in the vicinity of the carotenoid S_2 state.[20] Such arrangement was recently challenged by more advanced calculations carried out by Wormit and Dreuw[22] who used the Tamm−Dancoff approximation to time-dependent density functional theory and concluded that the precursor charge-transfer state is above the S_2 state of carotenoids and, consequently, cannot be involved in forming final charge-separated state. None of the abovementioned calculations reproduce the energy of the final charge-separated state expected from the redox potential of the Car^+-B800^- pair, suggesting that interaction with the protein

environment may push the precursor charge-transfer state below the S_2 state. Also, the $1B_u^-$ state[8,42] cannot be a priori excluded as a precursor of the charge-separated state, although its covalent nature suggests that it may be rather poor in donating electrons. In any case, the solution of this problem awaits further experimental and theoretical studies that may also reveal the function of the charge-separation event in LH2 complexes.

5. Conclusions

Application of transient absorption spectroscopy in combination with LDS treatment of LH2 complexes from purple bacteria containing carotenoids with different conjugation length provided information about the role of the B800 BChl*a* in carotenoid−BChl*a* energy and electron transfer. The main conclusions can be summarized as follows.

The B800 BChla is the major acceptor of energy from the S_1 state of carotenoids, accounting for ~60% of total S_1-mediated energy transfer. Interestingly, this value is virtually independent of conjugation length of the carotenoid donor, suggesting that a change in spectral overlap between the hypothetical carotenoid S_1 emission and B800 absorption band is not the only factor determining the energy transfer efficiency. The total efficiency of the S_1-mediated energy transfer decreases from 94 to 75% when going from neurosporene to spheroidenone, but the B800 BChl*a* remains the major energy acceptor despite that the S_1 emission has a better overlap with the lower-lying B850 BChl*a* for spheroidenone that has the lowest S_1 energy of all carotenoids studied here.

Perturbation of the B800 site by LDS treatment prevents formation of the carotenoid radical, confirming that B800 BChl*a* is the electron acceptor in the process of charge separation between carotenoid and BChl*a*. The carotenoid radical is formed only when B800 BChl*a* is present and only after excitation of the S_2 state of the carotenoid. Excitation of BChl*a*, even into the Soret band lying higher than the S_2 state of all carotenoids studied here, does not lead to formation of a carotenoid radical. The efficiency of the radical formation is higher for carotenoids with shorter conjugation length; for the longest studied carotenoid, spheroidenone, no radical formation was observed even with B800 BChl*a* present. On the basis of the radical formation time, 300−400 fs, the sub-100 fs lifetime of the S_2 state precludes this state to be a direct precursor of the radical formation. Since the radical signal exhibits linear dependence on excitation intensity, a possibility of radical formation via a nonlinear, multiphoton process involving some higher-lying states can be safely excluded. Instead, either hot S_1 or a charge-transfer state are suggested to play a role of the precursor of the charge-separated state.

Acknowledgment. Research in Czech Republic was supported by grants from the Czech Ministry of Education (MSM6007665808) and the Grant Agency of the Czech Academy of Sciences (IAA608170604). In the laboratory of H.A.F., this research is supported by the National Institutes of Health (GM-30353) and the University of Connecticut Research Foundation. The work at Lund University was supported by grants from the Swedish Research Council and the Wallenberg Foundation.

Supporting Information Available: Time course of the LDS-induced changes of absorption spectra and kinetics measured in the carotenoid radical region after excitation at 395 and 515 nm. This material is available free of charge via the Internet at http://pubs.acs.org.

References and Notes

(1) Polívka, T.; Sundström, V. *Chem. Rev.* **2004**, *104*, 2021.
(2) Frank, H. A.; Cogdell, R. J. *Photochem. Photobiol.* **1996**, *63*, 257.
(3) Ritz, T.; Damjanović, A.; Schulten, K.; Zhang, J.-P.; Koyama, Y. *Photosynth. Res.* **2000**, *66*, 125.
(4) Papiz, M. Z.; Prince, S. M.; Howard, T.; Cogdell, R. J.; Isacs, N. W. *J. Mol. Biol.* **2003**, *326*, 1523.
(5) Walz, T.; Jamieson, S. J.; Bowers, C. M.; Bullough, P. A.; Hunter, C. N. *J. Mol. Biol.* **1998**, *282*, 833.
(6) Gall, A.; Gardiner, A. T.; Cogdell, R. J.; Robert, B. *FEBS Lett.* **2006**, *580*, 3844.
(7) Sundström, V.; Pullerits, T.; van Grondelle, R. *J. Phys. Chem. B* **1999**, *103*, 2327.
(8) Koyama, Y.; Rondonuwu, F. S; Fujii, R.; Watanabe, Y. *Biopolymers* **2004**, *74*, 2.
(9) Rondonuwu, F. S.; Yokoyama, K.; Fujii, R.; Koyama, Y.; Cogdell, R. J.; Watanabe, Y. *Chem. Phys. Lett.* **2004**, *390*, 314.
(10) Papagiannakis, E.; Kennis, J. T. M.; van Stokkum, I. H. M.; Cogdell, R. J.; van Grondelle, R. *Proc. Natl. Acad. Sci. U.S.A.* **2002**, *99*, 6017.
(11) Papagiannakis, E.; Das, S. K.; Gall, A.; Stokkum, I. H. M.; Robert, B.; van Grondelle, R.; Frank, H. A.; Kennis, J. T. M. *J. Phys. Chem. B* **2003**, *107*, 5642.
(12) Papagiannakis, E.; van Stokkum, I. H. M.; Vengris, M.; Cogdell, R. J.; van Grondelle, R.; Larsen, D. S. *J. Phys. Chem. B* **2006**, *107*, 5727.
(13) Krueger, B. P.; Scholes, G. D.; Jimenez, R.; Fleming, G. R. *J. Phys. Chem. B* **1998**, *102*, 2284.
(14) Ricci, M.; Bradforth, S. E.; Jimenez, R.; Fleming, G. R. *Chem. Phys. Lett.* **1996**, *259*, 381.
(15) Desamero, R. Z. B.; Chynwat, V.; van der Hoef, I.; Jansen, F. J.; Lugtenburg, J.; Gosztola, D.; Wasielewski, M. R.; Cua, A.; Bocian, D. F.; Frank, H. A. *J. Phys. Chem. B* **1998**, *102*, 8151.
(16) Zhang, J.-P.; Fujii, R.; Qian, P.; Inaba, T.; Mizoguchi, T.; Koyama, Y.; Onaka, K.; Watanabe, Y. *J. Phys. Chem. B* **2000**, *104*, 3683.
(17) Polívka, T.; Pullerits, T.; Frank, H. A.; Cogdell, R. J.; Sundström, V. *J. Phys. Chem. B* **2004**, *108*, 15398.
(18) Macpherson, A. N.; Arellano, J. B.; Fraser, N. J.; Cogdell, R. J.; Gillbro, T. *Biophys. J.* **2001**, *80*, 923.
(19) Hsu, C.-P.; Walla, P. J.; Head-Gordon, M.; Fleming, G. R. *J. Phys. Chem. B* **2001**, *105*, 11016.
(20) Polívka, T.; Zigmantas, D.; Herek, J. L.; He, Z.; Pascher, T.; Pullerits, T.; Cogdell, R. J.; Frank, H. A.; Sundström, V. *J. Phys. Chem. B* **2002**, *106*, 11016.
(21) Walla, P. J.; Linden, P. A.; Hsu, C.-P.; Scholes, G. D.; Fleming, G. R. *Proc. Natl. Acad. Sci. U.S.A.* **2000**, *97*, 10808.
(22) Wormit, M.; Dreuw, A. *J. Phys. Chem. B* **2006**, *110*, 24200.
(23) Frank, H. A.; Brudvig, G. W. *Biochemistry* **2004**, *43*, 8607.
(24) Papagiannakis, E.; Stokkum, I. H. M.; van Grondelle, R.; Niederman, R. A.; Zigmantas, D.; Sundström, V.; Polívka, T. *J. Phys. Chem. B* **2003**, *107*, 11216.
(25) Chadwick, B.; Zhang, C.; Cogdell, R. J.; Frank, H. *Biochim. Biophys. Acta* **1987**, *893*, 444.
(26) Fraser, N. J.; Dominy, P. J.; Ücker, B.; Siminin, I.; Scheer, H.; Cogdell, R. J. *Biochemistry* **1999**, *38*, 9684.
(27) Cogdell, R. J.; Hipkins, M. F.; MacDonald, W.; Truscott, T. G. *Biochim. Biophys. Acta* **1981**, *634*, 191.
(28) Frank, H. A.; Bautista, J. A.; Josue, J.; Pendon, Z.; Hiller, R. G.; Sharples, F. P.; Gosztola, D.; Wasielewski, M. R. *J. Phys. Chem. B* **2000**, *104*, 4569.
(29) Zigmantas, D.; Hiller, R. G.; Sharples, F. P.; Frank, H. A.; Sundström, V.; Polivka, T. *Phys. Chem. Chem. Phys.* **2004**, *6*, 3009.
(30) Billsten, H. H.; Zigmantas, D.; Sundström, V.; Polívka, T. *Chem. Phys. Lett.* **2002**, *355*, 465.
(31) de Weerd, F. L.; van Stokkum, I. H. M.; van Grondelle, R. *Chem. Phys. Lett.* **2002**, *354*, 38.
(32) Jeevarajan, J. A.; Wei, C. C.; Jeevarajan, A. S.; Kispert, L. D. *J. Phys. Chem.* **1996**, *100*, 5637.
(33) Zhang, J.-P.; Skibsted, L. H.; Fujii, R.; Koyama, Y. *Photochem. Photobiol.* **2001**, *73*, 219.
(34) Gall, A.; Cogdell, R. J.; Robert, B. *Biochemistry* **2003**, *42*, 7252.
(35) Frank, H. A.; Bautista, J. A.; Josue, J. S.; Young, A. J. *Biochemistry* **2000**, *39*, 2831.
(36) Fujii, R.; Onaka, K.; Kuki, M.; Koyama, Y.; Watanabe, Y. *Chem. Phys. Lett.* **1998**, *288*, 847.

(37) Billsten, H. H.; Herek, J. L.; Garcia-Asua, G.; Hashøj, L.; Polívka, T.; Hunter, C. N.; Sundström, V. *Biochemistry* **2002**, *41*, 4127.
(38) Kosumi, D.; Komukai, M.; Hashimoto, H.; Yoshizawa, M. *Phys. Rev. Lett.* **2005**, *95*, 213601.
(39) Wohlleben, W.; Buckup, T.; Herek, J. L.; Cogdell, R. J.; Motzkus, M. *Biophys. J.* **2003**, *85*, 442.
(40) Zhang, J.-P.; Fujii, R.; Koyama, Y.; Rondonuwu, F. S.; Watanabe, Y.; Mortensen, A.; Skibsted, L. H. *Chem. Phys. Lett.* **2001**, *348*, 235.
(41) Pan, J.; Benkö, G.; Xu, Y.; Pascher, T.; Sun, L.; Sundström, V.; Polívka, T. *J. Am. Chem. Soc.* **2002**, *124*, 13949.
(42) Sashima, T.; Nagae, H.; Kuki, M.; Koyama, Y. *Chem. Phys. Lett.* **1999**, *299*, 187.